High power NIR fiber-optic femtosecond Cherenkov radiation and its application on nonlinear light microscopy

Ming-Che Chan[1,2,*] Chi-Hsiang Lien,[3] Jyan-Yo Lu,[1] and Bo-Han Lyu[1]

[1]*Institute of Imaging and Biomedical Photonics, College of Photonics, National Chiao-Tung University, Tainan City 71150, Taiwan*

[2]*Department of Medical Research, Chi Mei Medical Center, Tainan City 71004, Taiwan*

[3]*Department of Engineering Science, National Cheng Kung University, Tainan City 701, Taiwan*

**mcchan@nctu.edu.tw*

Abstract: We reported a record high power (>250 mW) and compact near-infrared fiber-optic femtosecond Cherenkov radiation source and its new application on nonlinear light microscopy for the first time (to our best knowledge). The high power femtosecond Cherenkov radiation was generated by 1.03 μm femtosecond pulses from a portable diode-pumped laser and a photonic crystal fiber as a compact, flexible, and highly efficient wavelength convertor. Sectioned nonlinear light microscopy images from mouse brain blood vessel network and rat tail tendon were then performed by the demonstrated light source. Due to the advantages of its high average output power (>250 mW), high pulse energy (>4 nJ), excellent wavelength conversion efficiency (>40%), compactness, simplicity in configuration, and turn-key operation, the demonstrated femtosecond Cherenkov radiation source could thus be widely applicable as an alternative excitation source to mode-locked Ti:Sapphire lasers for future clinical nonlinear microscopy or other applications requiring synchronized multi-wavelength light sources.

OCIS codes: (180.4315) Nonlinear microscopy; (190.4370) Nonlinear optics, fibers; (320.7110) Ultrafast nonlinear optics.

References and links

1. W. Denk, J. H. Strickler, and W. W. Webb, "Two-photon laser scanning fluorescence microscopy," Science **248**(4951), 73–76 (1990).
2. J. M. Squirrell, D. L. Wokosin, J. G. White, and B. D. Bavister, "Long-term two-photon fluorescence imaging of mammalian embryos without compromising viability," Nat. Biotechnol. **17**(8), 763–767 (1999).
3. N. G. Horton, K. Wang, D. Kobat, C. G. Clark, F. W. Wise, C. B. Schaffer, and C. Xu, "In vivo three-photon microscopy of subcortical structures within an intact mouse brain," Nat. Photonics **7**(3), 205–209 (2013).
4. S. Sakadzić, U. Demirbas, T. R. Mempel, A. Moore, S. Ruvinskaya, D. A. Boas, A. Sennaroglu, F. X. Kaertner, and J. G. Fujimoto, "Multi-photon microscopy with a low-cost and highly efficient Cr: LiCAF laser," Opt. Express **16**(25), 20848–20863 (2008).
5. M. E. Dickinson, E. Simbuerger, B. Zimmermann, C. W. Waters, and S. E. Fraser, "Multiphoton excitation spectra in biological samples," J. Biomed. Opt. **8**(3), 329–338 (2003).
6. S. P. Tai, M. C. Chan, T. H. Tsai, S. H. Guol, L. J. Chen, and C.-K. Sun, "Two-photon fluorescence microscope with a hollow-core photonic crystal fiber," Opt. Express **12**(25), 6122–6128 (2004).
7. S. H. Chia, C. H. Yu, C. H. Lin, N. C. Cheng, T. M. Liu, M. C. Chan, I. H. Chen, and C.-K. Sun, "Miniaturized video-rate epi-third-harmonic-generation fiber-microscope," Opt. Express **18**(16), 17382–17391 (2010).
8. R. Tanaka, S. Fukushima, K. Sasaki, Y. Tanaka, H. Murota, T. Matsumoto, T. Araki, and T. Yasui, "In vivo visualization of dermal collagen fiber in skin burn by collagen-sensitive second-harmonic-generation microscopy," J. Biomed. Opt. **18**(6), 061231 (2013).
9. R. M. Williams, W. R. Zipfel, and W. W. Webb, "Interpreting second-harmonic generation images of collagen I fibrils," Biophys. J. **88**(2), 1377–1386 (2005).
10. C. Zimmermann, V. Vuletic, A. Hemmerich, L. Ricci, and T. W. Hänsch, "Design for a compact tunable Ti:sapphire laser," Opt. Lett. **20**(3), 297–299 (1995).
11. P. St. J. Russell, "Photonic Crystal Fibers," Science **299**(5605), 358–362 (2003).
12. P. St. J. Russell, "Photonic-Crystal Fibers," J. Lightwave Technol. **24**(12), 4729–4749 (2006).
13. M. C. Chan, T. M. Liu, S. P. Tai, and C.-K. Sun, "Compact fiber-delivered Cr:Forsterite laser for nonlinear light microscopy," J. Biomed. Opt. **10**(5), 054006 (2005).

#206874 - $15.00 USD Received 20 Feb 2014; revised 3 Apr 2014; accepted 3 Apr 2014; published 11 Apr 2014

14. M. C. Chan, S. H. Chia, T. M. Liu, T. H. Tsai, M. C. Ho, A. A. Ivanov, A. M. Zheltikov, J. Y. Liu, H. L. Liu, and C.-K. Sun, "1.2-2.2 μm Tunable Raman Soliton Source Based on a Cr:Forsterite-Laser and a Photonic-Crystal Fiber," IEEE Photon. Technol. Lett. **20**(11), 900–922 (2008).
15. G. Chang, L.-J. Chen, and F. X. Kärtner, "Highly efficient Cherenkov radiation in photonic crystal fibers for broadband visible wavelength generation," Opt. Lett. **35**(14), 2361–2363 (2010).
16. X. M. Liu, J. Lægsgaard, U. Møller, H. H. Tu, S. A. Boppart, and D. Turchinovich, "All-fiber femtosecond Cherenkov radiation source," Opt. Lett. **37**(13), 2769–2771 (2012).
17. J. Takayanagi, T. Sugiura, M. Yoshida, and N. Nishizawa, "1.0-1.7-μm wavelength-tunable ultrashort-pulse generation using femtosecond Yb-doped fiber laser and photonic crystal fiber," IEEE Photon. Technol. Lett. **18**(21), 2284–2286 (2006).
18. G. P. Agrawal, *Nonlinear Fiber Optics* (Academic, 2007).
19. W. H. Lin, C. M. Chen, Y. C. Lan, and M. C. Chan are preparing a manuscript to be called "Numerical analysis of synchronized fiber-optic multiple wavelength converters through Cherenkov radiation and soliton-self-frequency shift."
20. M. T. Tsai and M. C. Chan, "Simultaneous 0.8, 1.0, and 1.3 μm multi-spectral and common-path broadband source for optical coherence tomography," Opt. Lett. **39**(4), 865–868 (2014).
21. J. C. Diels and W. Rudolph, *Ultrashort Laser Pulse Phenomena* (Academic, 1996)
22. J. Y Lu, C. W. Huang, J. C. Chen, and M. C. Chan are preparing a manuscript to be called "Energenic 1.3 μm Raman soliton source for multi-photon and multi-harmonic microscopy."
23. G. J. Tearney, R. H. Webb, and B. E. Bouma, "Spectrally encoded confocal microscopy," Opt. Lett. **23**(15), 1152–1154 (1998).
24. Y. Mao, S. Chang, E. Murdock, and C. Flueraru, "Simultaneous dual-wavelength-band common-path swept-source optical coherence tomography with single polygon mirror scanner," Opt. Lett. **36**(11), 1990–1992 (2011).
25. M. T. Myaing, J. Urayama, A. Braun, and T. B. Norris, "Nonlinear propagation of negatively chirped pulses: Maximizing the peak intensity at the output of a fiber probe," Opt. Express **7**(5), 210–214 (2000).
26. I.-H. Chen, S.-W. Chu, C.-K. Sun, P. C. Cheng, and B.-L. Lin, "Wavelength dependent cell damages in multi-photon confocal microscopy," Opt. Quantum Electron. **34**(12), 1251–1266 (2002).
27. A. Zumbusch, G. R. Holtom, and X. S. Xie, "Three-dimensional vibrational imaging by coherent anti-Stokes Raman scattering," Phys. Rev. Lett. **82**(20), 4142–4145 (1999).
28. C. W. Freudiger, W. Min, B. G. Saar, S. Lu, G. R. Holtom, C. W. He, J. C. Tsai, J. X. Kang, and X. S. Xie, "Label-Free Biomedical Imaging with High Sensitivity by Stimulated Raman Scattering Microscopy," Science **322**(5909), 1857–1861 (2008).
29. C. W. Freudiger, W. Yang, G. R. Holtom, N. Peyghambarian, X. S. Xie, and K. Q. Kieu, "Stimulated Raman scattering microscopy with a robust fibre laser source," Nat. Photonics **8**(2), 153–159 (2014).
30. S. W. Hell and J. Wichmann, "Breaking the diffraction resolution limit by stimulated emission: stimulated-emission-depletion fluorescence microscopy," Opt. Lett. **19**(11), 780–782 (1994).
31. H. C. Wang, Y. C. Lu, C. Y. Chen, C. Y. Chi, S. C. Chin, and C. C. Yang, "Non-degenerate fs pump-probe study on InGaN with multi-wavelength second-harmonic generation," Opt. Express **13**(14), 5245–5252 (2005).

1. Introduction

Since its first demonstration, nonlinear light microscopy (NLM), including multi-photon fluorescence microscopy [1–6] and multi-harmonic generation microscopy [7–9], has attracted much biological and medical interest due to its capability to provide molecular and structural information with high 3D spatial resolutions. Recently, enabled by femtosecond near-infrared (NIR) solid-state light sources working in the 0.7-1.3 μm bio-penetration window, NLM with a solid-state NIR light source offers the advantages of deeper penetration and much reduced photodamage and photobleaching effects [2, 4, 8].

Among the femtosecond NIR solid-state light sources, Kerr-lens mode-locked Ti:Sapphire lasers have become the gold standard in NLM [4]. With their working wavelength located in the 0.65-1.1 μm, femtosecond Ti:Sapphire lasers with energetic multi-nJ output pulse energies and femtosecond output pulse durations are excellent excitation sources for two-photon fluorescence (TPF) imaging because two-photon absorption spectra in most common biomedical labeling fluorophores are centered between 0.7 μm and 1 μm window [4]. Moreover, the widely wavelength tunability of mode-locked Ti:Sapphire lasers enables exciting two or more different labeling dyes in the same sample [5]. Thus, mode-locked Ti:Sapphire lasers have currently been widely adopted for basic research requiring maximum performances in the laboratory.

However, for pumping the Ti:Sapphire laser crystal, instead of the direct diode-pumping scheme, a high power 532 nm green laser, implemented by a complex intra-cavity frequency doubled 808 nm-diode-pumped 1064 nm Nd:YAG laser, is usually needed. Water-cooled systems, instead of air-cooled systems, are also needed for heat removal from Ti:Sapphire

#206874 - $15.00 USD Received 20 Feb 2014; revised 3 Apr 2014; accepted 3 Apr 2014; published 11 Apr 2014

crystals [10]. For wavelength tuning in Ti:Sapphire laser, precise and complicated opto-mechanical adjusting procedures are necessary. The bulky and complicated pumping, cooling, and wavelength tuning structures of femtosecond Ti:Sapphire lasers limit their use for future biomedical or even clinical applications.

Recently, by the invention of photonic crystal fibers (PCFs), fiber-dispersion and fiber-nonlinearity can be artificially engineered [11, 12]. By various PCFs, despite delivering femtosecond pulses with low temporal distortion [6, 7, 13], optical fibers can function as wavelength up-convertors by soliton self-frequency shift (SSFS) effect [3, 14] and wavelength down-convertors by Cherenkov radiation (CR) [15–17] nonlinear process. Accordingly, for future biomedical and clinical NLM applications requiring compact femtosecond source within the 0.7 to 1 μm window, an alternative light source to current mode-locked Ti: Sapphire laser can be implemented by combining a compact/portable/turn-key-operated femtosecond laser working outside the 0.7 to 1 μm window as pump and a proper PCF as an efficient/low-cost/easily-operated/direct-diode-pumped wavelength convertor. The fiber-delivered light source, composed of a compact femtosecond pump laser and a PCF-based wavelength convertor, breaks the wavelength limitation arising from the bandwidth of laser gain medium. And the fiber-output can be directly connected to the nonlinear microscope, which results in a more compact system arrangement, a better isolation from environmental noises than bulk-optics-based beam delivery systems [7, 13], a good spatial beam quality and a natural compatibility to endoscope system [7].

In the reported fiber-delivered light source with a wavelength down convertors to longer wavelength by the SSFS effect, Xu's group has demonstrated a 1.7 μm frequency-shifted Raman soliton source by a high-power 1.55 μm Erbium-doped fiber laser and a large-mode PCF [3]. The energetic Raman soliton was then utilized for deep-brain imaging. However, limited by the area theory of solitons [3, 18] and currently available wavelength-conversion fibers, below the 1.3 μm spectral window (especially in the short wavelength regime), energetic fiber-delivered Raman soliton source, defined as a femtosecond soliton source with a more than 1 nJ pulse energy, is still a challenge for laser physicist and engineer [3, 14, 18].

On the other hand, toward shorter wavelength regime, in the reported fiber-delivered femtosecond source with a wavelength up convertors through the CR effect, generating high power femtosecond CR pulses are theoretically possible but there were few experiment reports on the fiber-delivered femtosecond CR sources [15–17] in the visible range. In 2010, Chang and his collabrators have demonstrated an excellent work of the CR generation by a home-made state-of-art 10-fs mode-locked Ti:Sapphire laser as a pump and a NL-1.8-710 PCF as a wavelength convertor [15]. A highly efficient (>40%) CR with a maximum 325 pJ pulse energy in the 0.4-0.5 μm wavelength regime was reported. On the other hand, by a compact Yb-doped fiber laser and a nonlinear fiber, Liu et al. have reported a 0.58-0.63 μm CR radiation maximum 4.8 mW power [16] and Nishizawa's group have demonstrated a 0.6-0.68 μm anti-Stoke radiation with a maximum 1 mW power together with an excellent 1.0-1.7 μm Raman soliton [17]. According to the reported average power and laser repetition rate [15–17], the calculated pulse energies were on the order of 0.1 nJ, which were more than an order-of-magnitude smaller than those required for clinical NLM imaging.

In this paper, based on the highly efficient CR effects of 1.03 μm femtosecond pulses inside a nonlinear PCF, we report a compact, portable, maintenance-free, and fiber-delivered 0.6-0.8 μm femtosecond light source. Power-dependent output characteristics of the CR source with different PCF lengths were also measured and analyzed. We observed that the central wavelength of CR can be easily tuned by simply adjusting the pump power in the PCF. Sectioned TPF images from mouse brain blood vessel network and second harmonic generation (SHG) images of rat tail tendon were performed by the demonstrated light source. Due to the advantages of its excellent wavelength conversion efficiency (>40%), high average output power (>250 mW), wavelength tunability over 100 nm, compactness, simplicity, and turn-key operation, for NLM, the demonstrated femtosecond CR source could thus be widely applicable as an alternative of mode-locked Ti:Sapphire laser in many clinical, biomedical, industrial or other applications.

#206874 - $15.00 USD Received 20 Feb 2014; revised 3 Apr 2014; accepted 3 Apr 2014; published 11 Apr 2014

2. Experimental setup

Figure 1 shows the schematics of the reported compact 0.6 to 0.8 μm femtosecond CR source (in the dashed box) and the related nonlinear microscope system. The CR source was composed of a 1.03 μm air-cooled Ytterbium femtosecond laser (Mikan, Amplitude Systems) as the excitation source and a nonlinear PCF (SC-3.7-975, NKT Photonics) as an efficient wavelength up-convertor. An optical isolator was inserted between the 1.03 μm femtosecond laser and nonlinear PCF to block backward reflection into the laser cavity which will destroy the mode-locking of laser. The laser footprint was as small as 18 × 33 cm with a high portability and turn-key operations. Throughout entire experiment where hundreds of TPF and SHG images with different conditions were acquired within several hours, the laser output and alignment opto-mechanics were kept stable because the observed image quality from the NLM remains stable. This experiment of NLM image acquisition within one day shows that short-term stability of the demonstrated femtosecond CR source was on the order of several hours. The realignment procedure can be done within 5 minutes between successive startups or within 10 minutes after the 1.03 μm femtosecond source has been moved, which indicates that the long-term stability of the light source was also good for future clinical applications. The zero dispersion wavelength of the nonlinear PCF was 975 nm and the dispersion value at 1.03 μm was around 13 ps/nm/km. The end of PCF fiber, playing a role as delivery fiber and wavelength convertor, was directly connected to the input end of a home-made scanning system as shown in the remaining part of Fig. 1. A fiber-delivered multi-modality nonlinear microscope, including TPF and SHG microscope, was then built up based on the first demonstrated 0.6-0.8 μm femtosecond CR light source. This system included galvanometer x-y scanners (6215H, Cambridge, USA) and an inverted optical microscope (Axiovert 200, Zeiss, Germany). All optics in the inverted microscope were modified to allow the passage of 600-1000 nm NIR light. With a 2-D scanner and an oil-immersion objective (40 × , numerical aperture (NA) = 1.3, Carl Zeiss), laser beams were sequentially focused into the samples and the generated nonlinear signals were collected, band-pass filtered, and detected by the photomultiplier tubes (PMTs) (H5783P, Hamamatsu, Japan). In this manner, imaging with nonlinear optical signals such as TPF and SHG can be achieved. The TPF and SHG wavelength was double confirmed with a fiber optic spectrometer.

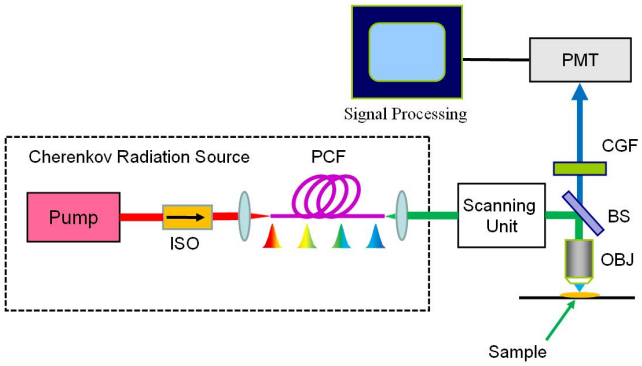

Fig. 1. Schematics of the 0.6-0.8 μm Cherenkov radiation (CR) light source (enclosed in the dashed box) and related nonlinear microscope system. The light source was composed of a compact 1030 nm femtosecond laser as excitation source and a nonlinear fiber as an efficient wavelength convertor. Pump: Compact 1030 nm Ytterbium-doped femtosecond laser; ISO: optical isolator; PCF: photonic crystal fiber; BS: beam splitter; OBJ: microscope objective; CGF: Colored glass filter; PMT; photomultiplier tube.

#206874 - $15.00 USD Received 20 Feb 2014; revised 3 Apr 2014; accepted 3 Apr 2014; published 11 Apr 2014

3. Numerical evaluation of the fiber-optic CR source

According to the theory of fiber-optic CR [18], the central wavelength of the CR is determined by the following nonlinear phase-matching equation:

$$\sum_{n\geq 2}\frac{(\omega_{CR}-\omega_P)^n}{n!}\beta_n(\omega_P)=\frac{\gamma P_P}{2} \quad (1)$$

where ω_{CR} and ω_P represent the central frequency of CR and the input 1.03 μm pump pulse. β_n are the nth order derivative of propagation constant at the 1.03 μm wavelength. γ and P_p represent the nonlinear fiber parameter and the pulse peak power, respectively. As shown in Fig. 2, according to the experimental condition of nonlinear fiber and pump pulse which will be described later in the Sec. 4 of this paper, the central wavelength of CR at different power levels was first numerically solved according to Eq. (1) where the polynomial order, n, was up to 9 [19], which is the least order to accurately describe the experimental nonlinear pulse propagation behaviors. In other words, the dispersion parameters of the nonlinear fiber, β_2 to β_9, were first numerically fitted and the 9-th-order polynomial was numerically solved by Mathematica software. The black line in Fig. 2 represents the phase-matching condition of CR wavelength as the function of pump wavelength without nonlinear phase term, $\frac{\gamma P_P}{2}$. At the 1.03 micron excitation with ~250 fs pulsewidth, the phase-matching CR wavelength from the simulation is located at 0.80 μm. On the other hand, the red, yellow, green and blue lines in Fig. 2 show the selected simulation of power-dependent central wavelength of the CR at fiber exit. As the pump power inside the fiber is 100mW, the central wavelength of CR is 0.77 μm. With the increase of launched power inside fibers, the central wavelength of CR decreases monotonously. Finally, for the pump power reaching 1000mW, the central wavelength of CR is 0.69 μm.

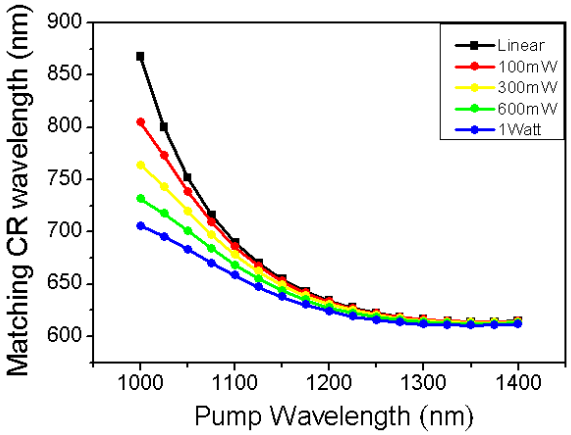

Fig. 2. Simulated linear phase-matching curve (black line) and nonlinear phase matching condition curves (red, yellow, green and blue lines) as the function of pump wavelength and pump power according to Eq. (1). The CR wavelength can be calculated via the phase-matching curve.

Due to the fact that the numerical simulation demonstrate the similar trends with our experimental results shown later in Fig. 4(d), for evaluating the CR generation by other femtosecond pump source and nonlinear wavelength conversion fiber, the method described in this section could be a simple evaluation method before performing experiments. Moreover, despite adjusting the pump power into PCFs, as shown in Fig. 2, the CR wavelength can also be tuned by varying the wavelength of the femtosecond pump. For calculating the more-detailed pulse propagation behaviors, various methods for solving the

#206874 - $15.00 USD Received 20 Feb 2014; revised 3 Apr 2014; accepted 3 Apr 2014; published 11 Apr 2014

nonlinear Schrodinger equations will be needed [18], which could be an interesting research topic in the future.

4. Experimental characterization of the high-power fiber-optic CR source

Figure 3(a) and its inset show the output spectrum of the 1.03 μm femtosecond pump laser and the related auto-correlation measurement. The Ytterbium laser emitted 250 fs pulses at a 1.03 μm central wavelength and a 6 nm full-width-half-maximum (FWHM) bandwidth. Typical average output power before the isolator and fundamental repetition rate of the excitation laser were 1W and 54.77 MHz, respectively. The output laser pulses were delivered into a piece of nonlinear PCF with different lengths where 1.03 μm femtosecond laser pulses were efficiently wavelength up-converted in the 0.6 to 0.8 μm range.

In NLM, the pulsewidth of the excitation source is one of the most important key parameters because the pulse broadening effect will degrade the excitation efficiencies of nonlinear signals in NLM. According to the literature [6], with the same pulse energy, the excitation efficiencies of TPF and SHG are inversely proportional to the pulse-width. For the demonstrated fiber-optic CR source, due to the fact that CR is always located in the normal-dispersion wavelength region of the nonlinear fiber [15–18], the generated femtosecond CR experiences severe pulse broadening when propagating through the optical fiber. Therefore, it is very important to find a proper fiber length for CR conversion. The fiber length should be long enough to generate CR but cannot exceed the length where the dispersion-induced pulse broadening effect is severe.

In this experiment, to experimentally find the optimum fiber length, several nonlinear PCFs with different lengths were utilized as the nonlinear wavelength conversion fiber. The power-dependent output spectra of a 40-cm nonlinear PCF were first measured as shown in Fig. 3(b). We experimentally observed the central wavelength of CR emission can be tuned from 0.76 to 0.66 μm by simply adjusting the pump power into the 40-cm nonlinear PCF [20]. However, due to the severe pulse-broadening in the 40-cm nonlinear PCF, the auto-correlation traces and NLM cannot be experimentally performed with the demonstrated CR light source shown in Fig. 3(b) where the a 40 cm PCF was adopted.

According to Fig. 3(b), in order to perform NLM, instead of a 40 cm PCF, finding a minimum required PCF length for generating CR without severe pulse-broadening effect was performed in the following experiment. The length of PCF was sequentially shortened to find the optimum required fiber length. Figure 3(c) shows power-dependent spectra of nonlinear PCFs with lengths of 20 cm. The central wavelength of CR emission can be tuned from 0.76 to 0.66 μm by simply adjusting the pump power into the 20-cm nonlinear PCF. The similar wavelength tuning ranges between the 40-cm PCF and 20-cm PCF shows that the CR pulses mainly experienced pulse-broadening effect in the last 20cm fiber. And the length of the nonlinear PCF should be further cut to diminish the pulse broadening effect.

Figure 3(d) shows power-dependent spectra of nonlinear PCFs with lengths of 8.5 cm. At a 100 mW pump power, the blue shift components in the spectrum were observed and we attributed them to CR, self-phase modulation, cross-phase modulation and four-wave mixing [18]. A blue-shifted CR was noticed at a central wavelength of 0.79 μm. As the power increase from 200mW to 650mW, the central wavelength of apparently CR emission can be tuned from 0.74 to 0.66 μm.

From Figs. 3(c) and 3(d) showing power-dependent spectra of nonlinear PCFs with lengths of 20 cm and 8.5 cm, similar wavelength tunability by adjusting the pump power into the fiber was also observed. In contrast, no CR radiations were observed at the ends of a 5 cm and a 7 cm PCF. We attribute it to the fact that the positively-chirped femtosecond pulses, originating from the dispersion of laser cavity and optical isolator, were compressed in the first 7 cm fiber and generating Cherenkov effects in the remaining fiber. Therefore, in this experiment, we can conclude that the minimum fiber length for generating CR is 8.5 cm. And from previous discussions, the optimum PCF length for NLM was also 8.5 cm where the blue-shifted CR was generated and the pulse-broadening effects were not too severe to degrade the excitation efficiencies of nonlinear signals. As shown in Fig. 3(d), when the

#206874 - $15.00 USD Received 20 Feb 2014; revised 3 Apr 2014; accepted 3 Apr 2014; published 11 Apr 2014

average power of 1.03 μm excitation pulses was increasing from 100 to 650 mW, the central wavelength of the emitted CR in the 8.5 cm fiber was shifted from 0.79 to 0.67 μm.

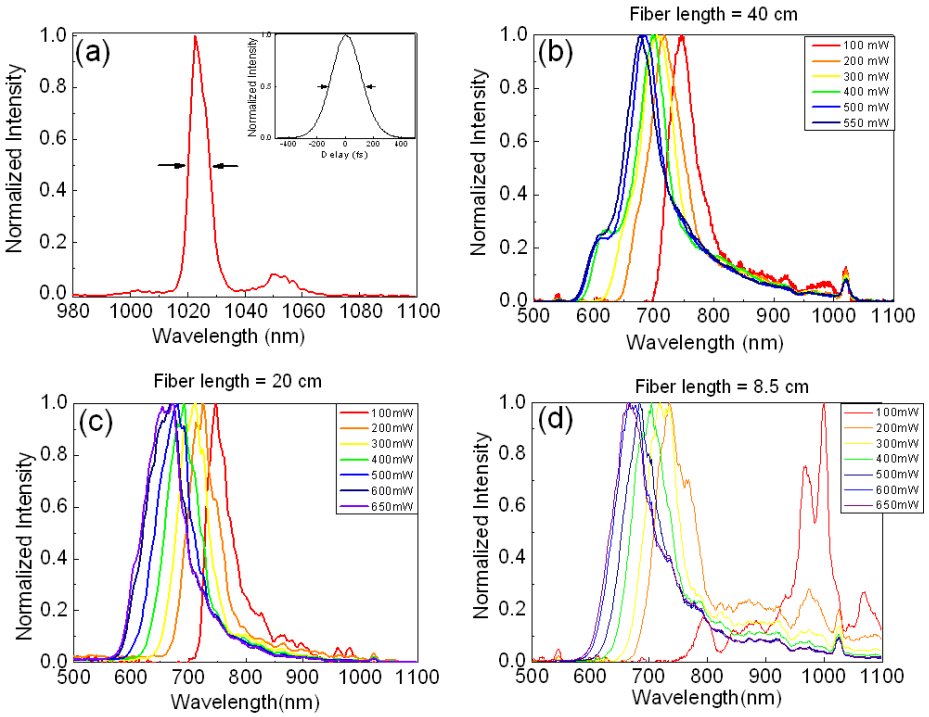

Fig. 3. (a) The output spectrum and auto-correlation traces (inset) of the pump 1.03 μm excitation laser. (b)~(d): Power-dependent CR spectra at the end of the (b) 40 cm PCF [20], (c) 20 cm PCF, and (d) 8.5 cm PCF.

To characterize the pulse-width of the generated high power femtosecond CR, Fig. 4(a) shows selected auto-correlation traces were measured at the end of the 8.5 cm PCF when the pump powers were 100, 200, 400, and 600 mW. Corresponding central wavelengths of CR emissions in Fig. 4(a) were 0.79, 0.74, 0.70, and 0.67 μm and the measured power-dependent pulse widths for the generated CR radiations were 905, 804, 562, and 404 fs, respectively. According to Fig. 3(d), the bandwidths of the 0.79, 0.74, 0.70, and 0.67 μm CR radiations were 16.3, 36.7, 43.8, and 48.7 THz. Thus, the calculated time-bandwidth products of the 0.79, 0.74, 0.70, and 0.67 μm CR were 6.585, 20.63, 35.21, and and 44.073 respectively. Since the time-bandwidth product of a transform-limited Gaussian pulse was 0.441 [21], the generated CR femtosecond pulses were far from transform-limited and thus have much room to be further compressed down to sub-50 fs regime by an external compressor, such as an piece of air-core PCF, a grating pair, or a prism pair. And the pulse compression will be helpful for enhancing the image quality of the signal to noise ratio at a given nonlinear laser scanning microscope [6]. Together with the generation of CR, the generation of SSFS in the 1.1-1.5 μm range and the residual pump pulse in the 1.03 μm range at the end of an 8.5 cm nonlinear PCF were also observed in this experiment [22]. The experimental observation shown in Fig. 3(d) is in good agreement of with our simulation shown in Fig. 2.

Besides the issue of pulsewidth, as an excitation source for NLM, the averaged power of the fiber-optic femtosecond CR source is also a key issue because NLM with a higher power source can increase the signal-to-noise ratio which reduces the image acquisition time and avoids motion artifacts. In order to measure the power characteristics and related conversion efficiencies of CR emissions, a high-quality dichroic beam splitter (F875-Di01-25x36, Semrock), with an 98% averaged reflectivity in 350 – 860 nm and an 93% transmission in

#206874 - $15.00 USD Received 20 Feb 2014; revised 3 Apr 2014; accepted 3 Apr 2014; published 11 Apr 2014

895-1600 nm, was selected and inserted after the fiber to separate the CR and the other emission spectra including residual 1.03 μm pump pulse and 1.1-1.5 μm SSFS. We consider the power distributed below 860 nm being carried on by CR because the isolated CR spectrum appears in this region in all the experiment cases. The average powers of CR measured at the end of a 40, 20 and 8.5 cm fiber were shown in solid blue, green, and red lines of Fig. 4(b). According to the measured CR powers, the calculated CR efficiencies, defined as measured power of CR divided by total pump power from PCF fiber, are shown in the dashed blue, green, and red lines of Fig. 4(b) respectively. Three dashed curves in Fig. 4(b) regarding the CR conversion efficiency follow the same trend: the CR conversion efficiency increases quickly with the addition of pump launched power and tends to saturate at higher power levels. From our simulations [19], the input 250 fs pulse formed a high-order solitons whose soliton order is equal to 5. Then the high-order solitons experienced soliton pulse compression during propagation. The compressed pulse width in our simulation was down to 59 fs. The soliton pulse compression effect is helpful to increase the wavelength conversion efficiency of CR, as described in [15]. The experimental curves on CR powers and CR efficiencies indicate that CR can be highly efficient (>40%) process with high average power (> 200 mW) and high pulse energy (>4 nJ) in all cases. Moreover, with the length increment of nonlinear PCF, the CR conversion efficiency slightly grows up and the threshold of CR was reduced. Please note that in this work the wavelength was adjusted by tuning the launched power inside PCFs. With a given nonlinear PCF and excitation laser, adjusting the chirp and polarization state of the incident light are alternative ways to tune the wavelength of CR because the nonlinear effects inside fibers can be changed by varying these two parameters [16]. In addition, for generating CR outside the 0.6-0.8 μm regime, it can be simply implemented by replacing another nonlinear PCF with different dispersion and nonlinear characteristics and follow the steps described in Sec. 3 to numerically calculate the wavelength of CR.

For some biophotonic end applications such as wavelength-encoded confocal microscope [23] or spectroscopic optical coherence tomography [20, 24], because the pulse-width is not the key issue, the fiber-optic CR source with a long wavelength-conversion PCF was preferred because of the reduced threshold of pump power and higher wavelength conversion efficiencies. On the other hand, for NLM, the femtosecond pulse broadening is related to the degradation of nonlinear signals [6, 24]. In this experiment, for NLM application, shorter PCF (8.5 cm) was selected as wavelength convertor because the pulse-broadening effect was diminished, which degraded excitation efficiencies of nonlinear signals, such as TPF and SHG, were partially recovered.

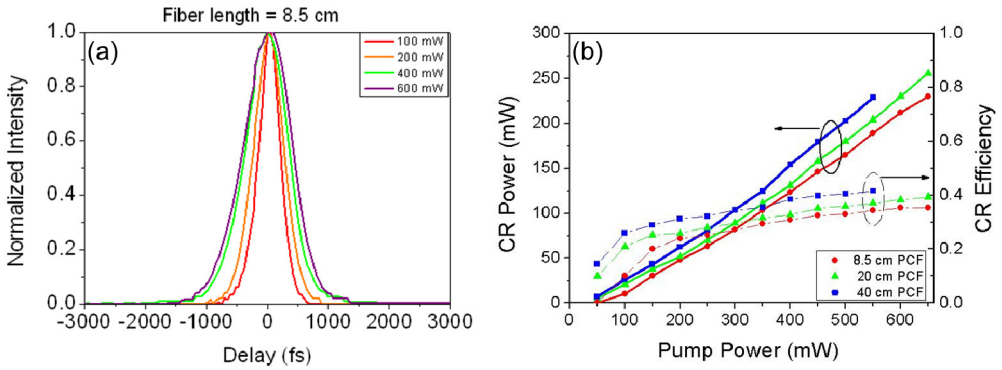

Fig. 4. (a) The power-dependent pulsewidth measurements at the end of the 8.5 cm PCF. The values inserted in the figure represent the total average pump power after the PCF. (b) The average power of CR (solid-lines) and corresponding CR conversion efficiency (dashed-lines) of 40 cm (blue-rectangular), 20 cm (green-triangle), and 8.5 cm (red-circle) PCF as the function of pump power.

#206874 - $15.00 USD Received 20 Feb 2014; revised 3 Apr 2014; accepted 3 Apr 2014; published 11 Apr 2014

5. Application of the NIR CR source on nonlinear light microscopy

To demonstrate the feasibility of femtosecond fiber-optic CR used as the nonlinear microscopy light source, several bio-samples had been adopted. In this demonstration, an 8.5 cm wavelength-conversion PCF was utilized in the CR source as discussed before. For the compactness issue of this CR light source, the output of the CR with a 120 mW average power (400 mW total output power) and a 0.70 μm central wavelength was directly connected to the nonlinear microscope without any external pulse compression components.

Figure 5 shows 3-D TPF imaging of fluorescence tissues and SHG imaging of rat tail tendon based on the CR source. In the TPF microscopy, we demonstrated the fluorescence tissue image by the mouse brain sections labeled with a stain for blood vessels (DiI). During measurement of one optical section, the field of view size was 100 μm with 512 pixels by 512 pixels. For reconstructing 3D image, each optical sectioning image was recorded at different position of the z axis by moving the position of the objective. In here, the sectioned images show the morphology and distribution of the blood vessel at shifting 5 μm of z step between each other in the Fig. 5(a). The blood vessel network was reconstructed by the same optical sectioning condition at each 1μm location with 100 μm depth in the Fig. 5(b).

On the other hand, SHG is a tool as a label free maker for visualizing the biological tissue [8, 9]. The rat tail tendon contains well aligned fibers/fibrillars of the rich type I collagen with strong SHG signal. Herein, we demonstrated the 50 μm by 50 μm square SHG image of the rat tail tendon in PBS (Phosphate buffered saline), which from an adult rat sacrificed as part of animal training exercises performed at the Laboratory Animal Center of National Cheng Kung University, as shown in the Fig. 5(c). In order to improve the good contrast, the pixel scanning rate setup at 1 kHz with 512 pixels by 512 pixels during the measurement. The image indicated a lot of small fibers/fibrillars are clear and intact inside the huge fiber of the tendon.

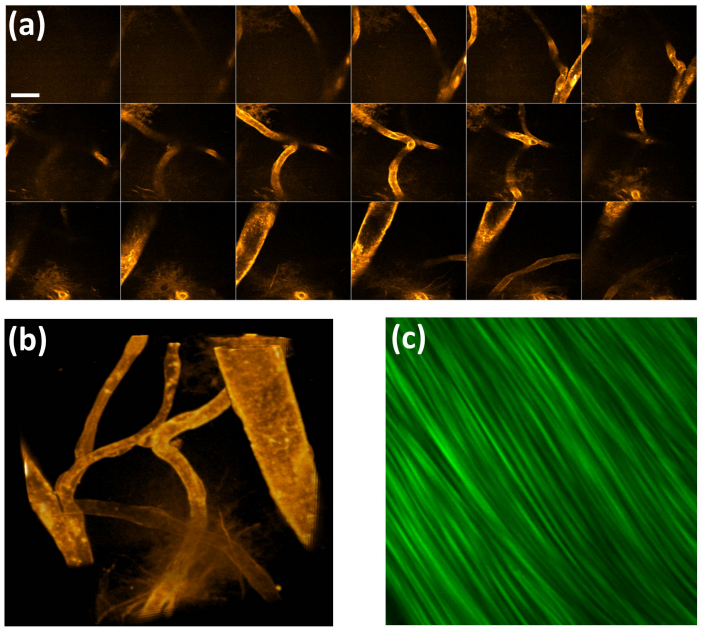

Fig. 5. (a) Sectioned two-photon fluorescence images (TPF) of blood vessels in mouse brains with different z depth. The length of scalar bar is 25 μm and the z-step size is 5 μm. (b) Reconstructed blood vessel network of the mouse brain in 3D space (Media 1). (c) Second harmonic generation image (SHG) of rat tail tendon in Phosphate buffered saline. Image size: 50 μm by 50 μm.

#206874 - $15.00 USD Received 20 Feb 2014; revised 3 Apr 2014; accepted 3 Apr 2014; published 11 Apr 2014

The image performance based on the demonstrated record high power femtosecond CR source is comparable with that based on commercially available Ti: Sapphire lasers in the 0.6~0.8 μm wavelength regime. According to [6], the image quality of the two-photon fluorescence and second-harmonic generation is proportional to the square of the excitation power. And the maximum average power on the sample at the 0.6-0.8 μm wavelength was limited to ~10 mW, corresponding to a 0.2 nJ pulse energy, due to sample viability and photo-bleach effects [26]. On the other hand, with the same pulse energy, the image quality in the nonlinear light microscope is inversely proportional to the pulse width [6, 27]. At a given nonlinear laser scanning microscope, the most efficient way to increase the signal to noise ratio is de-chirping the femtosecond CR pulse after the PCF.

6. Discussions and conclusions

In this work, we have proposed and demonstrated a novel scheme of nonlinear microscopy by the fiber-optic femtosecond CR with high conversion efficiencies and record high output power. The wavelength of CR can be numerically evaluated in advance by the method we described in Sec. 3 in this paper. The fiber-optic CR source can be implemented for other end applications requiring additional excitation wavelength by simply replacing the wavelength conversion fiber where the fiber dispersion and nonlinear parameters can be artificially engineered. The fiber-output femtosecond CR can be directly connected to the input of end application to provide the compact and flexible beam delivery. Based on the fiber-optic output CR, a new application on nonlinear light microscopy was demonstrated for the first time (to our best knowledge). This preliminary demonstration in NLM shows that the compact fiber-delivered light source with turn-key operation can be now utilized for clinical diagnosis and have the potential for future endoscopic imaging as described In [7] since the fiber-optic output is compatible with endoscope system.

Due to the fact that the generated femtosecond CR from the output of the wavelength conversion fiber is synchronized with the original pump pulse, besides the applications of multi-photon and multi-harmonic generation microscopy demonstrated in this work, with carefully control the relative spatial and temporal properties of the two synchronized femtosecond pulses, the demonstrated light sources are very useful for future novel biomedical applications, such as coherent Raman scattering (CARS) microscopy [27], stimulated Raman (SRS) microscopy [28, 29], stimulated emission depletion (STED) microscopy [30], and multi-color pump-probe microscopy [31].

In conclusion, for NLM, we demonstrate a compact and wavelength tunable femtosecond fiber-delivered CR source in 0.6-0.8 μm wavelength ranges as an alternative excitation source of mode-locked Ti:Sapphire lasers. This source was composed of an ultra-compact 1.03 μm air-cooled Ytterbium femtosecond laser as the excitation and a nonlinear PCF as an efficient wavelength convertor. Sectioned TPF images from mouse brain blood vessel network and SHG images from rat tail tendon were performed by the demonstrated light source. Due to the advantages of its excellent wavelength conversion efficiency (>40%), high average output power (>250 mW), wavelength tunability over 100 nm, simplicity, compactness, and turn-key operation, the demonstrated femtosecond CR source shows great potential for future NLM applications.

Acknowledgments

The authors acknowledge Prof. Shean-Jen Chen of National Cheng Kung University for loaning some experimental instruments. The authors also acknowledge the scientific discussions with Dr. Hung-Wen Chen of Massachusetts Institute of Technology, Prof. Chi-Kuang Sun of National Taiwan University and Dr. Li-Jin Chen of Thorlabs. This research was supported in part by the National Science Council of Taiwan, ROC (NSC 100-2221-E-009-092-MY3) and the Department of Medical Research, Chi Mei Medical Center, Tainan 71004, Taiwan.